USING NON-ADIABATIC EXCITATION TRANSFER FOR SIGNAL TRANSMISSION BETWEEN MOLECULAR LOGIC GATES

A. I. Martynov[a], A. S. Belov[b] and V. K. Nevolin[a]
[a] National Research University of Electronic Technology, 1 Shokin Square, Zelenograd, Moscow, Russia
[b] Department of Chemistry, Lomonosov Moscow State University, 1-3 Leninskie gory, Moscow, Russia
`e-mail: amartinov@edu.miet.ru`

ABSTRACT

Molecular logic gates (MLG) are molecules which perform logic operations. Their integration into a computing system is a difficult task which remains to be solved. The problem lies in the field of signal exchange between the gates within the system. We propose using non-adiabatic excitation transfer between the gates to address this problem while absorption and fluorescence are left to communicate with external devices. Excitation transfer was studied using the modified Bixon-Jortner-Plotnikov theory on the example of the 3H-thioxanthene-TTF-dibenzo-BODIPY covalently linked triade. Several designs of the molecule were studied in vacuum and cyclohexane. It was found that the molecular logic system has to be planar and rigid to isolate radiative interfaces from other gates. Functioning of these gates is based on dark $\pi\sigma^*$-states in contrast to bright $\pi\pi^*$-states of radiative interfaces. There are no fundamental differences between $\pi\pi^* \rightarrow \pi\sigma^*$ and $\pi\pi^* \rightarrow \pi\pi^*$ transitions for cases when an exciton hops from one gate to another. The rates of such transitions depend only on an energy gap between states and distance between gates. The circuit is highly sensitive to the choice of solvent which could rearrange its state structure thereby altering its behavior. According to the obtained results, non-adiabatic transfer can be considered as one of the possible ways for transmitting a signal between MLGs.

***K*eywords** Molecular logic gate; MLG; Rate constant; non-adiabatic transfer; the Bixon-Jortner-Plotnikov method

1 Introduction

In the last two decades researchers have been wondering whether molecular logic gates (MLGs) can be integrated into a circuit [1, 2, 3, 4, 5, 6]. Currently, it is possible to assemble simple cascades which include only two or three gates [7, 8, 9, 10, 2, 11]. Building a complex logic system like a processor is yet to be done. The fact is that an MLG is a molecular sensor which has a complex response to environment. This response is determined by the rules similar to logic operations. Inputs and outputs often have different nature, exhibit quantum properties, cannot reach target inputs or trigger side reactions [5]. It is necessary to overcome these challenges for creating a complex molecular logic system (MLS). Researchers managed to make a lot of simple devices, such as AND, XOR, INH gates, half adders and keypad lock [12, 13], but they can operate only as individual sensors. To become a component of a circuit, a device should be able to exchange signals. The question is, what kind of signal carrier is most suitable to minimize the negative effects mentioned above. Such a signal carrier would make it possible to create molecular circuits.

Some molecular gates use chemical species as signal carriers [8, 9, 10, 7]. MLGs were initially developed as molecular sensors which react to protons and ions in the medium. A natural extension is to create an MLG which releases chemical species at output, while another MLG receives these species as input. There were reports of cascades of gates in which the signal carrier was a proton [10], an ion [8, 9] or other species [7, 14]. In this approach a circuit is as a sequence of chemical reactions [15]. One can use different types of reactions depending on the task, even irreversible ones [16]. In chemical MLSs, all molecules of the same type play the role of individual logic gates while molecules of another type together form the other gate. External influence makes molecules of the first type to release ions, and the signal is passed when concentration of ions reaches the certain threshold value. Only after that the second-type gates react to this. Thus, chemical signalling does not allow to transmit a signal between individual gates.

Another type of MLGs uses photons for signaling instead of chemical species. They do not take part in chemical reactions but only absorb and emit light. All-photonic gates do not require addition of chemical reagents, there is no accumulation of reaction products, occurring processes are reversible, there is no diffusion which limits the rate: delay can be as small as several femtoseconds [5]. For signal transmission, the absorption spectrum of a receiving gate must overlap with the fluorescence spectrum of a transmitting gate. The signal reaches the target gate with high probability if the transmitting and receiving gates are physically connected by a short linker. Förster resonance energy transfer (FRET) takes place if the distance between molecules is less than 50 $\hat{A}$[17]. Due to this phenomenon, energy is transferred between molecules if their electronic states are in resonance. Using this property, Wagner built large molecular wires from Zn-porphyrins [18, 19, 20]. This phenomenon was used also for connecting MLGs [2], but in this case a cascade includes no more than three gates [21]. Guliev [2, 21] used mixed type gates which operate with optical and chemical signals. He showed that linking does not change functional purpose of MLGs, but makes the signal transfer more effective. Levine used this phenomenon for creating a full-adder on the basis of rhodamine 6G and azulene[22],in which each molecule is a self-sufficient MLG which works as a all-photonic half-adder. After integration they exchange signals through FRET-channel, so that the system works as a full-adder. All-photonic MLGs have many interesting properties well described in Budyka's review [5].

There are three main types of setups of all-photonic gates. The first setup (fluorophore-quencher) is also frequently used for creating chemical gates. All-photonic gates differ in that they switch between turn 'on' and 'off' states under irradiation but not due to capture of chemical species. Light changes the structure of a quencher resulting in its molecular orbitals shifted which leads to the change in ability to pull electrons and therefore quench excitation. This setup allows to make several simple gates such AND and INHIBIT [23]. The second setup was proposed by Kompa and Levine [24]. They considered the lowest excited states of some abstract molecule as a basis for constructing a half-adder. The resulting MLG had two inputs and two outputs at different wavelengths. The concept of Kompa and Levine allows building an MLG based only on the structures of electronic states. For an MLG to perform a desired operation, one needs to design a molecule with a certain order of electronic states [22, 25, 26, 27, 11]. This allows one to abstract from molecular geometry and paves the way to algorithmic development of MLGs. The third setup is based on on singlet fission (SF) and triplet–triplet annihilation (TTA) [28]. Light irradiation generates an exciton which goes through series of singlet and triplet states. This construction is similar to the Kompa-Levine gate in the aspect that its functioning is determined by its electronic structure. On the other side, this setup does not require high-energy excited states. Moreover, such a gate allows to receive input photons one not at the same time, but in turn. All setups of gates can be building blocks of an excitonic circuit.

The main advantage of all-photonic gates which allows to assemble them into a circuit is also a disadvantage. For a logic circuit to work properly, its components have to exchange signals only with the gates they are connected to, according to the logic scheme of the device. On the other hand, FRET acts at distances less than 50 $\hat{A}$ and links all the gates whose spectra overlap [17]. If signal exchange occurs via FRET, all gates can receive the incoming signal with some probability which leads to parasitic signal transmission and complicates handling of an MLS. The widths of absorption spectral bands of molecules usually lie in the range of tens and hundreds of nanometers. It is possible that spectral bands of internal gates of an MLS could overlap with the bands of receiving antennas. Thus, there is a need for gates which do not interact with light but have the advantages of all-photonic gates.

An MLS should be kept in the dark so that internal gates could not be triggered by an incident photon. Even if the molecule is isolated from external noise, gates can emit and absorb photons themselves. To avoid such problems, one should divide an MLS into an external and internal subsystem. The former is to absorb input and produce output photons while the latter should be able only to process the signal but not to interact with visible radiation. The signal exchange between the two subsystems has to proceed only in a non-radiative way. Hudson et al. proposed a similar framework in which internal subsystem works on triplet excited states. The signal exchange proceeds via SF and TTA mechanisms. We, in turn, proposed to use a dark singlet excited states between which an exciton moves non-adiabatically [29].

We tested the possibility of non-radiative signal transmission between moieties of a molecule via non-adiabatic coupling [29]. To disengage from logical processes of a molecular gate, the test system was based on YES-gates, the simplest logic gates which pass the signal unchanged. The cascade of YES-gates was implemented physically as a chain of tetrathiafulvalene (TTF) moieties. The first excited state S_1 of each moiety has $\pi\sigma^*$-character making it almost dark. The chain has a manifold of dark excitonic states which are localized at their respective moieties. These states lie lower than other electronic states and form an excitonic band of the molecule. Localization is provided by –CN and –F substituents which remove degeneracy and form an enery gradient between units. The gradient ensures that an exciton moves from one end of the chain to the other unidirectionally. There were examples in which an exciton moves faster than decay by two orders of magnitude. The work [29] shows that the internal system can work according to the requirements stated above.

To confirm the viability of the proposed system, one needs to study how the external and internal subsystems work together. The TTF-chain from earlier work[29] can serve only as a signal conductor because it cannot receive an external signal. There are no antennas of the external subsystem which can receive or transmit signal. In this work we study the functioning of a simple system: receiver-(YES-gate)-transmitter. Ideally, the receiver had to absorb a photon and transform it into an exciton, which would pass through the YES-gate to the transmitter. The latter is there to convert the exciton back into a photon with a longer wavelength. Both the receiver and the transmitter have to have the first excited state whose energy is close to that of the first excited state of TTF. The energy of the receiver should be higher than the energy of TTF, while the latter should be higher than the energy of the transmitter. Frontier orbitals of all fragments should be at the same level, otherwise charge transfer states would interfere with signal transmission. Moreover, the $S_1 \rightarrow S_0$ transitions of terminal moieties must have very high oscillator strength. In view of these considerations, 3H-thioxanthene is a suitable option for the role of the receiver, while dibenzo-BODIPY is suitable for the transmitter. In result, the model molecule is a 3H-thioxanthene-TTF-dibenzo-BODIPY triad. Several ways to connect the moieties were studied giving rise to structures denoted as ‘Chain’, ‘Line’ and ‘S-line’ (Fig. 1). Kinetics of transitions between excited states was studied for each molecule in vacuum and in cyclohexane. To build their kinetic models, non-adiabatic rate constants were calculated for the transfer between each state of interest. Separability of the system into two subsystems for rate calculations was tested on these models.

In contrast to previous attempts of integration MLGs into a system, gates exchange signals non-adiabatically. This feature allows to shield some gates from interaction with light, while letting other gates absorb and emit photons. In this work, we studied theoretically the signal exchange between two types of gates which differ in character of their excited states (π or σ). Dynamics of such system has been investigated using the example of the 3H-thioxanthene-TTF-dibenzo-BODIPY molecule. This study looked at the effects of environment and molecular design. Rate constants in vacuum and cyclohexane were calculated using the Bixon-Jortner-Plotnikov theory. The obtained rates were used for building a kinetic model which has been tested for aptness with an ideal system receiver-(YES-gate)-transmitter.

2 Theory

Since the internal gates exchange signals through a non-adiabatic channel, a theory which describes such transitions is needed.

A sample molecule has a manifold of electronics states: the ground state and several excited ones. Several lowest excited states are localized at their respective moieties. An exciton moves through the chain by hopping between moieties. The theory used can describe exciton hopping between two units, and the Hamiltonian for this process is

$$\hat{H} = E_i |i\rangle \langle i| + E_f |f\rangle \langle f| + V_{if} |i\rangle \langle f| + V_{fi} |f\rangle \langle i| \tag{1}$$

where E_i and E_f are the energies of the initial $|i\rangle$ and final $\langle f|$ electronic states, while V_{if} and V_{fi} are non-diagonal parts of Hamiltonian corresponding to transitions between states.

In general, a wave function of the molecule is a superposition of $|i\rangle$ and $|f\rangle$. The function consists only of the component $|i\rangle$ initially, but the contribution of $|f\rangle$ increases over time until the wave function becomes $|f\rangle$ completely. If the system is viewed in terms of state populations, their time evolution can be described by the master equation - a set of first-order kinetic equations with time-independent rate constants. The constant for the tranisition from state $|i\rangle$ to state $|f\rangle$ can be calculated by the Fermi Golden Rule[30] as follows:

$$k_{if} = \frac{2\pi}{\hbar} \sum_{mn} |V_{mn}|^2 \delta(E_{if} - E_n + E_m) \tag{2}$$

where $E_{if} = E_i - E_f$ is the transfer energy, V_{mn} is a perturbation causing the transition $|i\rangle |m\rangle \rightarrow |f\rangle |n\rangle$, in which m and n denote vibronic levels of the molecule $n = \{n_1, n_2 \ldots n_{(3N-6)}\}$ where N is the number of atoms.

The rate constants of non-adiabatic transfer can be calculated using Bixon-Jortner-Plotnikov formula [31, 32, 33]. It applies to cases where anharmonicity and the Dushinsky effect are negligible [31] and where a molecule in the initial electronic state is in the 0-th vibronic level. Such conditions are most relevant for a rigid molecule at near-zero absolute temperature. After transition, the molecule is in one of multiple states whose energies are near the transfer energy E_{if}. Despite that the model takes into account only one vibronic level of $|i\rangle$, all vibronic levels of the $|f\rangle$-state should be considered.

Full enumeration of all vibronic levels which meet the requirements is an NP-complete task. An additional challenge is that a level is involved in the process only if its energy is close to E_{if}. Moreover, there are no clear criteria for

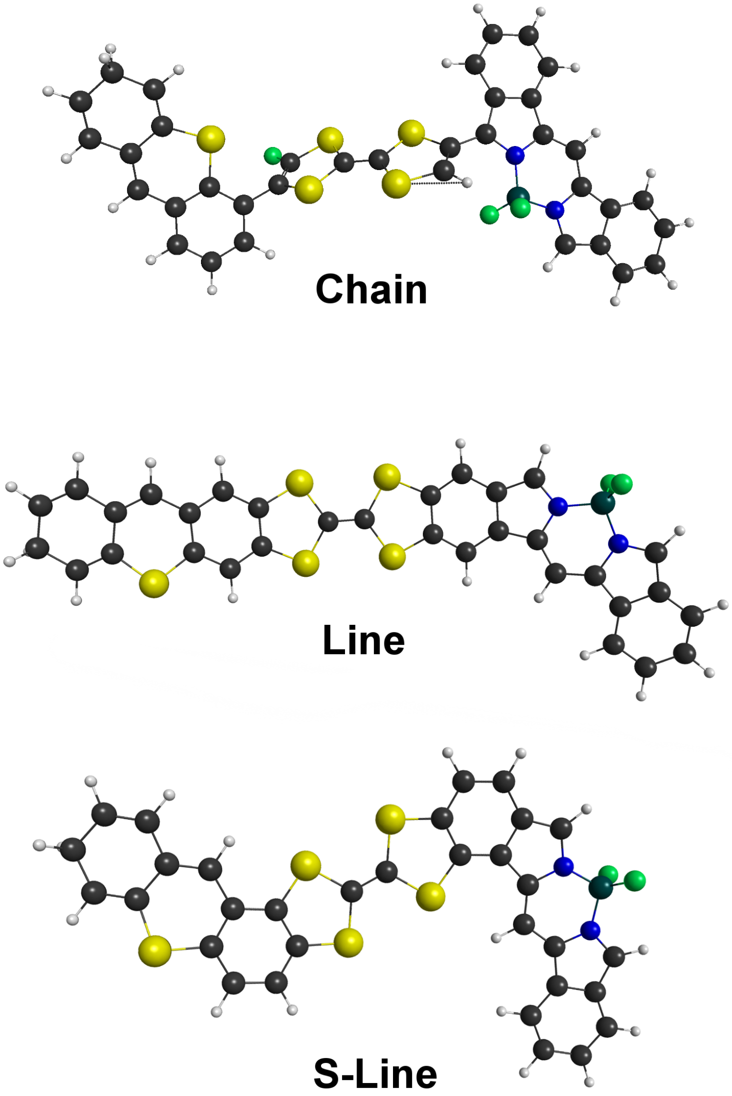

Figure 1: The model molecules ‘Chain’, ‘Line’ and ‘S-line’ based on 3H-thioxanthene, TTF and dibenzo-BODIPY. Hydrogen is shown in white, boron - dark green, nitrogen - blue, carbon - black, fluorine - green, sulfur - yellow.

selection of active (promoting) levels. To overcome this problem, several approximations are in use, among which the Marcus approximation[30] is the most popular. However, it is relevant only for transitions with a small E_{if}. The larger is the transfer energy, the worse the approximation works. In the general case, we can use the Pekarian function for approximating the density of states for calculation of non-adiabatic transfer rates [34].

$$\begin{aligned} k_{IC} = \frac{\pi}{\hbar}\sum_j |\Theta_j^Q|^2 \omega_j e^{-y_j} \sum_{n_j=0}^{\infty} \frac{(n_j-y_j)^2 y_j^{n_j-1}}{n_j!} D_j(E_{if}-\hbar n_j\omega_j) \\ + \frac{\pi}{\hbar}\sum_j \Theta_j^Q \sqrt{\omega_j} e^{-y_j} \sum_{v\neq j} \Theta_v^Q \sqrt{\omega_v} e^{-y_v} \times \sum_{n_j=0}^{\infty} |n_j-y_j| \frac{y_j^{n_j-1}}{n_j!} \\ \times \sum_{n_v=0}^{\infty} |n_v-y_v| \frac{y_v^{n_v-1}}{n_v!} D_{jv}(E_{if}-\hbar(n_j\omega_j+n_v\omega_v)) \end{aligned} \tag{3}$$

where j, v are vibronic modes, n_j and n_v are the numbers of vibronic modes, ω_j is the frequency of j-th mode, y_j is the Huang-Rhys factor, θ_j^Q is the non-adiabatic coupling constant between $|i\rangle$ and $|f\rangle$ projected onto the j-th mode in normal coordinates, $D_j(E)$ is the effective density of states, during the construction of which the j-th mode was excluded, $D_{jv}(E)$ is the effective density of states, during the construction of which the j-th and v-th modes were excluded.

Many quantum chemical programs can calculate the non-adiabatic coupling Θ_j^Q only for transitions from the excited state to the ground one at the TD-DFT level of theory. Calculation of the coupling between excited states is unavailable for TD-DFT. On the other hand, those programs can find the coupling between excited states at the MCSCF level of theory, but combining the values obtained by two different methods has its drawbacks. First, it is not entirely correct to use different levels of theory for evaluating parameters of the same function. Second, the computational cost of MCSCF increases very fast with the size of a molecule and an active space. For our molecules, calculation becomes unfeasible for active spaces which would ensure an acceptable accuracy. Thus, it would be advisable to calculate the non-adiabatic coupling between excited states at the TD-DFT level of theory.

The non-adiabatic coupling can be found approximately via

$$\Theta_j^Q = \frac{\langle i|\partial U/\partial Q_j|f\rangle}{E_f - E_i} = \sum_v M_v^{-1/2} A_{vj} \frac{\langle i|\partial U/\partial R_v|f\rangle}{E_f - E_i} \tag{4}$$

where E_i and E_f are the energies of the $|i\rangle$ and $|f\rangle$ states respectively, U is the potential energy, M_v is the mass of the v-th atom, R_v is a Cartesian coordinate, A_{vj} is matrix for transforming the Cartesian coordinates into the normal ones. The integral $\langle|\partial U/\partial R_v|\rangle$ is the potential of a Coulomb field which can be calculated by many quantum chemistry programs [35]. It can be calculated, in particular, at the TD-DFT level of theory, which provides methodological consistency to this study.

In the general case, the density of states is given by[30]

$$D_{\pm}(E-E_{if}) = -\frac{1}{2\pi\hbar i}\int dw \exp\left(G(w) - G(0) \pm w(E-E_{if})/\hbar\right) \tag{5}$$

$$G(w) = \sum_j y_j[(1+b(\omega_j))e^{w\omega_j} + b(\omega_j)e^{-w\omega_j}]$$

where $G(w)$ is the correlation function, $w = -it$, while $b(\omega)$is the Bose-Einstein distribution, the sign ± indicates the direction in which the processes occurs: '+' is for fluorescence, '-' is for absorption.

In the Pekarian approximation, the formula has the form[36, 34]

$$D_{\pm}(E-E_{if}) = \sum_z \frac{1}{\sqrt{2\pi|g''(w_{2z})|}} \exp\left(g(w_{2z})\right) \tag{6}$$

where

$$g(w) = G(w) - G(0) \pm w(E - E_{if})/\hbar$$

The parameter w_z is calculated in two steps. Firstly, approximate values are found using formulas derived by Pekar and Krivoglaz[36]. Secondly, the precise values are calculated using gradient descent method[34].

The theory outlined above describes non-adiabatic transfer in vacuum, while an environment may contribute to the rate. To account for that, the solvent surrounding the molecule was introduced into the model as a set of harmonic oscillators which mediate the relaxation of excited states. Since their mode characteristics cannot be calculated directly,the Debye spectral function $\mathcal{J}_D(\omega)$ was used to take into account the contribution of the environment.

The manifold of vibronic levels of the environment is quasi-continuous, therefore we can replace the summation with integration in the formula (5) and replace the Huang-Rhys factors with the spectral function $\mathcal{J}(\omega)$. Then, the correlation function of a solvent $G_S(w)$ becomes [30]

$$G_S(w) = \int d\omega \cdot \mathcal{J}(\omega)[(1 + b(\omega))e^{w\omega} + b(\omega)e^{-w\omega}] \tag{7}$$

Then we can equate the spectral function $\mathcal{J}(\omega)$ to the Debye function $\mathcal{J}_D$, which depends on the reorganization energy of the solvent E_λ and the Debye frequency ω_D. The reorganization energy can be obtained from calculation, while the Debye frequency can be extracted from experimental data. This frequency is equal to $2.19 \cdot 10^{-4}$ Hartree (or 69K)[37].

$$\omega \cdot \mathcal{J}_D(\omega) = \theta(\omega)\frac{2E_\lambda}{\pi\hbar}\frac{\omega_D}{\omega^2 + \omega_D^2} \tag{8}$$

Substituting $\mathcal{J}_D(\omega)$ into $G(w)$ gives [30]

$$G_S(w) = G_1(w) - iG_2(w)$$

where

$$G_1(w) = -\frac{2k_B T E_\lambda}{(\hbar\omega_D)^2}(e^{-iw\omega_D} + iw\omega_D - 1) \tag{9}$$

$$G_2(w) = \frac{E_\lambda}{\hbar\omega_D}(1 - e^{-iw\omega_D}) \tag{10}$$

The total correlation function is composed of correlation functions of the molecule and the environment. We replaced the molecule correlation function by the total one in formula (6). Because of that, the formula for the density of states becomes:

$$D_\pm(E - E_{if}) = \frac{1}{2\pi\hbar}e^{-G(0)}\int dw \cdot e^{G(w)+G_1(w)-iG_2(w)\pm w(E-E_{if})/\hbar} \tag{11}$$

Accordingly, the inclusion of the enviroment in the model affected the Pekarian formula

$$D_\pm(E - E_{if}) = \sum_z \frac{exp\{g(w_{2z}) + G_1(w_{2z}) - iG_2(w_{2z})\}}{\sqrt{2\pi|g''(w_{2z}) + G_1''(w_{2z}) - iG_2''(w_{2z})|}} \tag{12}$$

To find the non-adiabatic rate for a molecule in a solvent, one needs to substitute (12) into (3). There, the designation $D(E_{if}) = D_+(0 - E_{if})$ is introduced for convenience. The new formula requires not only the parameters of the molecule but also the parameters of the solvent, such as ω_D and E_λ. The last one can be found using formula [30]

$$E_\lambda = F_f(P_i) - F_f(P_f) \tag{13}$$

This formula reflects how the coupling $F_f(P)$ between the molecule and the solvent changes after transition. The subscript f means that the molecule is in the f-th electronic state. The parameter P takes into account the polarization of the solvent around the molecule. When the molecule is in the i-th state, the solvent has the polarization P_i. In the final

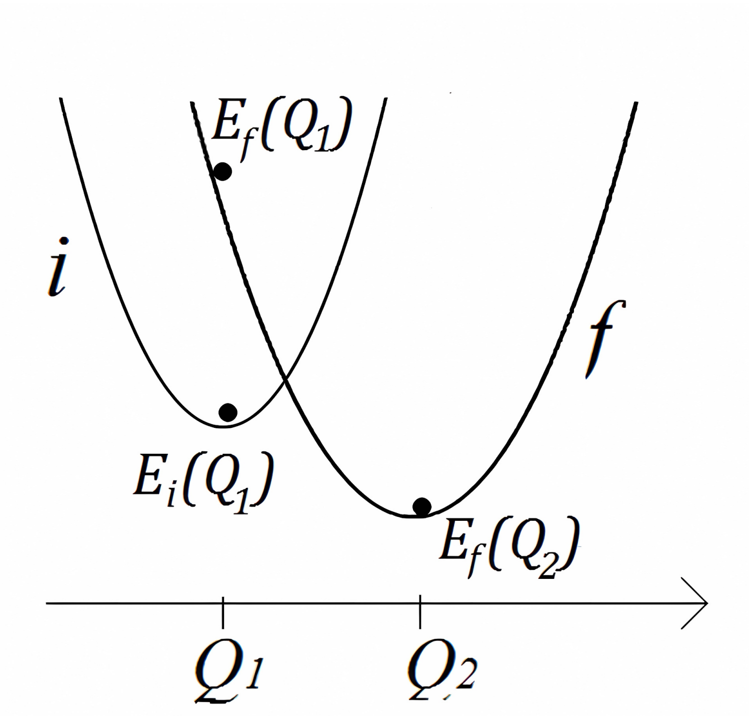

Figure 2: Schematic PESes of the initial and final states.

electronic state f the polarization equals P_f. The first term $F_f(P_i)$ of the formula (13) reflects the energy of the system which has changed its electronic states $i \to f$, but the polarization remains unchanged P_i. The second term $F_f(P_f)$ corresponds to the case in which the solvent has adapted itself to the new state of the molecule. Existing software tools can calculate the reorganization energy for ionization. Since this calculation can be performed only at DFT level of theory, but not TD-DFT, we need an alternative method to calculate the reorganization energy.

We developed the simple technique for evaluating the reorganization energy which uses the energy of the molecule in vacuum E^V, the energy of the molecule in the solvent E^S, the solvation energy F, which equals to a difference between the two other energies $F = E^S - E^V$ (Fig. 2). This allows working with two limiting cases. In the first case, the transfer $i \to f$ occurs so slowly that the solvent has enough time to adapt to a new Columbic field of the molecule. This is the limit of slow transfer, for which the reorganization energy is given by

$$E_\lambda^{Slow} = F_i(Q_1) - F_f(Q_2) = (E_i^S(Q_1) - E_i^V(Q_1)) - (E_f^S(Q_2) - E_f^V(Q_2)) \tag{14}$$

The opposite case is the limit of fast transfer in which only the electronic component of polarization has the time to adapt, while the orientation component remains unchanged. The reorganization energy in this limit can be calculated using the formula

$$E_\lambda^{Fast} = F_i(Q_1) - F_f(Q_1) = (E_i^S(Q_1) - E_i^V(Q_1)) - (E_f^S(Q_1) - E_f^V(Q_1)) \tag{15}$$

The permittivity depends on the field frequency since the total polarizability of a dielectric consists of orientation and electronic polarizabilities. Orientation of molecules matters at frequencies lower than 10^6 Hz. This component ceases to be relevant in the range from 10^6 to 10^9 Hz because molecules do not have enough time to rotate. The permittivity depends only on the electronic polarizability at frequencies higher than 10^9 Hz[38]. If a transfer lasts longer than 1 μs, the slow limit occurs. The fast limit is relevant for transfers which are faster than 1 ns. When dealing with a particular system, it is convenient to calculate the rate constant in both limits. After this, one can choose the result which is within the range of applicability of the theory.

Let us now address the rates of radiative transfers. One has to evaluate their contribution to the kinetics in the system to complete the picture. In the harmonic limit, the rate of fluorescence has the form[31]

$$k_{Rad} = \frac{f_{os} \nu_{if}^2}{1.5} \tag{16}$$

where f_{os} is the oscillator strength, ν_{if} is the frequency of transition expressed in cm^{-1}. The numerical value has the dimension of inverse seconds (s^{-1}) and does not need additional conversion.

While only the rate constants are interesting for non-radiative transfer, radiative transfer is also characterized by spectrum of this transition. The spectrum of fluorescence has the form[30]

$$I(E) = \frac{4E^2}{3c^3\hbar^2} |d_{if}|^2 D_+(E - E_{if}) \tag{17}$$

where d_{if} is the dipole moment of transition, c is the speed of light, $D(E)$ is the density of states which is the same as for non-radiative transfer. The formula (6) is relevant for vacuum, and the formula (12) is relevant for a molecule in a solvent.

The absorption spectrum can be modeled using the formula[30]

$$\alpha(E) = \frac{4\pi^2 E n_{mol}}{3c\hbar} |d_{if}|^2 D_-(E - E_{if}) \tag{18}$$

where n_{mol} is the number of molecules which take part in the process.

A convenient way to describe the width of a spectral band is the full width at half maximum (FWHM). Assuming the Gaussian shape of the band, this parameter has the value

$$FWHM = 2\sqrt{2\ln 2 \sum_i y_i \omega_i^2 (2b(\omega_i) + 1)} \tag{19}$$

where ω_i is the frequency of the i-th mode, y_i is the Huang-Rhys factor, $b(\omega)$ is the Bose-Einstein distribution.

Taking into account influence of the solvent, formula has a form

$$FWHM = 2\sqrt{2\ln 2 (\sum_i y_i \omega_i^2 (2b(\omega_i) + 1) + 2k_B T E_\lambda)} \tag{20}$$

in which the term $k_B T$ is obtained from $G_S(w) \approx 2k_B T$ for $\omega_D w \ll 1$. All formulas described in this section are relevant for the cases in which anharmonicity and the Dushinsky effect are negligible [31, 36]. If the system meets these requirements, a PES can be calculated only from equilibrium coordinates and a Hessian. According to this, Penfold and Eng[39] developed a method for controlling that a transition meets the requirements of the Franck–Condon (FC) approximation. One needs to know the exact gradient elements κ_j of the final state which can be calculated *ab initio*, and the gradient elements κ_j^* within harmonic approximation which can be evaluated via the formula

$$\kappa_j^* = \omega_j^2 (Q_j^i - Q_j^f) \tag{21}$$

The applicability of the FC approximation can be tested by the parameter Ξ

$$\Xi = \frac{K_+ - K_-}{k_+} \times 100\% \tag{22}$$

where

$$K_+ = Max(\sum_j^{3N-6} |\kappa_j|, \sum_j^{3N-6} |\kappa_j^*|)$$

$$K_- = Min(\sum_j^{3N-6} |\kappa_j|, \sum_j^{3N-6} |\kappa_j^*|)$$

If the molecule meets the requirements of the FC approximation, the parameter is zero: $\Xi = 0$. If a transition is accompanied by strong distortion, the parameter is close to 100%. A transition can be considered a FC transition if $\Xi < 10\%$. Although higher values of Ξ are not the evidence of an incorrect result, they are the reason to proceed with caution.

The formulas provided above are necessary for calculation of the rate constants of transitions between states. The kinetic behavior of the system was studied as follows. Firstly, electronic states of interest were selected. Secondly, *ab initio* parameters were calculated and used to find the rate constants according to the formulas above. Then, kinetics in the system was modeled based on these constants. Each studied system was checked for meeting the following set of requirements. An exciton must pass through the sequence of gates before it recombines, decays into an electron-hole pair or spreads over several gates losing its localized character. The states of internal gates have to be dark and not mix with bright states of the external system. The quantum efficiency should be as large as possible (preferably >0.9). The medium should be robust with respect to heat dissipated in the process. For the system to be controllable, it is necessary that it should have a separate spectral range for excitation of the input gates without exciting other gates. As a result of this work, it is shown that a photonic molecular logic system can have a subsystem within which communications occur non-adiabatically.

3 Computational details

The non-radiative transfer rates were calculated using an in-house program[34, 40] which checked the requirements of the FC approximation using the formula (22) and then calculated the non-adiabatic transfer rates in vacuum (3, 6) or in solvent (3, 12) for certain E_λ and ω_D. The program also produced absorption and fluorescence spectral profiles using formulas (17,18) and calculated the value of the FWHM parameter (19, 20). The rates of radiative transitions were evaluated manually by using the formula (16). The in-house program used ab initio parameters of the studied molecules to perform calculations.

The input parameters were calculated using GAMESS ver 30 sep 2020 (R2)[41]. The geometries of sample molecules were optimized at DFT or TD-DFT[42] levels of theory using camb3lyp/sbkjc(f)[43] in the Tamm-Dancoff approximation[44]. Energies, potential of electric field, moments d_i of states, oscillator strength f_{osc} of transitions, Hessians of the ground states were calculated at the same level of theory. The gradients of the $|f\rangle$ state were found at the equilibrium geometry of the $|i\rangle$ state. For solvated molecules, this data was recalculated using the pcm/smd model[45, 46]. The non-adiabatic coupling was evaluated via potential of an electric field using the formula (4)

The parameters E_{if} and E_λ were calculated as follows. In vacuum, the parameter E_{if} is just the difference between the initial and final states for transition. The parameter E_λ is not needed for an isolated molecule. For the molecule in a solvent, E_{if} and E_λ were found in several steps. Firstly, one had to obtain equilibrium geometries in the solvent for the initial and final states (Q_i^S and Q_f^S). The superscript 'S' implies that the parameters were calculated for the molecule surrounded by the solvent at the TD-DFT/camb3lyp/smd level of theory. The manifold of solvated energies of electronic states $E_i^S(Q_i^S)$ and $E_f^S(Q_f^S)$ were calculated for these geometries. After this, the energies in vacuum $E_{Ex}^V(Q_i^S)$ and $E_{Ex}^V(Q_f^S)$ were calculated for these geometries at the TD-DFT/camb3lyp level of theory. Major excitations contributing to the excited states were identified to establish correspondence between electronic states in vacuum and in solvent. The parameter E_{if} was the difference between the solvated energies:

$$E_{if} = E_i^S(Q_i^S) - E_f^S(Q_f^S) \tag{23}$$

The reorganization energy was calculated using the formula (14) or (15) depending on the rate regime: 'slow' or 'fast'.

The non-radiative and radiative rates were used for building a model of the system. Each model included the lowest exciton state for each unit and other states in this energy range. It was assumed that an exciton is located at the 3H-thioxanthene moiety at the initial moment of time. The behavior of the system was studied in regards with state populations and quantum efficiency of exciton passing through the molecule. Additionally, controllability and heat effects were analyzed.

4 Results and Discussion

The *ab initio* parameters of the ground and lowest excited states were calculated for the molecules studied. For transitions between states, the FC approximation validity criterion Ξ, the radiative k_{Rad} and non-radiative k_{IC} rates, full width at half maximum (FWHM) of these spectra were found, both for the molecule in vacuum and in cyclohexane. The non-radiative rates k_{IC} in the solvent were calculated both in the 'slow' and 'fast' limit. However, the rates were the same

Table 1: Energies and dipole moments of electronic states for the ‘Chain’ molecule in *vacuum*. The energy of the ground state is chosen as the zero level.

State	Configuration	Energy (eV)	Moment (D)
e1	●−○−○	2.898	5.628
e2	○−●−○	2.499	4.451
e3	○−○−●	2.468	3.319
e4	○−⊕−⊖	2.003	13.697
e0	○−○−○	0.0	2.375

for all transitions, so we provide only one value of a non-adiabatic rate for each transition. Since the theory is based on the Fermi golden rule, it can be applied only for irreversible transitions between weakly coupled distinguishable states. If, due to the time-energy uncertainty principle, two states are indistinguishable, we consider that the transition is beyond limits of applicability. Such transitions are marked with an asterisk (*).

Electronic states of the studied molecules will be denoted hereinafter as follows. The molecule is represented by three circles (○−○−○) or (○○○), in which the leftmost one stands for 3H-thioxanthene, the second is TTF, and the last one denotes dibenzo-BODIPY. The white circle (○) indicates that a moiety is not excited, the black circle (●) stands for an exciton located at a moiety. If a moiety has lost an electron, it has a ⊕ sign, while the fragment which has received an electron has a ⊖ sign. The tables 1, 2, 5, 6, 9 and 10 provide energies and dipole moments of the considered states. The dipole moments of solvated molecules do not include cavity surface charge.

The analysis of the obtained results for each case followed the general pattern. Firstly, we compared the rates of transitions between various states. The difference between recombination rates at various moieties is important to assess if the system was appropriately divided into the internal and external parts. Secondly, we were interested in FWHM of spectral lines because it determines the bandwidth of a state which serves as a window for excitation. Selectivity of excitation depends on how much these windows overlap with each other. Thirdly, we evaluate the non-adiabatic transfer rates because they determine exciton behavior. For a reliable system functioning it is required that these rates are higher than relaxation and recombination rates. The aggregate of these parameters is the basis for analyzing the viability of an MLS, both the external and internal subsystems.

4.1 Chain

Only the first four excited states are relevant in the context of the task for the ‘Chain’ molecule. Those include three exciton states localized on one of the moieties. The fourth state has a charge-transfer character and lies lower than other states. The type of each state was identified according to the dominating configuration and the dipole moment (Fig. 3 and 4). The design of the molecule ensures that the energies of states form a ladder which sets the direction of exciton movement (Tables 1 and 2). The charge transfer state (CT) was not planned as an essential part of the model but it appeared as the last state in the sequence. This state is due to an accidental proximity of dibenzo-BODIPY LUMO energy to that of the HOMO of TTF. Despite this, ‘Chain’ can be used as a model of a simple MLS.

A surprising fact is that the environment affects the energies of the exciton states more than CT states. The exciton states form a narrow band with a width of 0.4 eV (Table 1) in vacuum, while the CT state lies lower than this band by 0.5 eV. The relative position of the CT state remains unchanged in cyclohexane. However, the solvent increases the width of exciton states band to 0.7 eV. The states (○●○) and (○○●) are shifted down by the solvent stronger than the (●○○) state. The domination configuration of the (●○○) state is the (HOMO-1→LUMO+1) transitionwith coefficients 0.966 for vacuum and 0.981 for cyclohexane. The (○●○) state mainly consists of the (HOMO→LUMO+2) and (HOMO→LUMO) configuration transitions. Under solvent influence coefficient of the (HOMO→LUMO+2) configuration decreases from 0.72 to 0.61, while the (HOMO→LUMO) configuration remains with a coefficient of 0.34. The (○○●) state includes the (HOMO-2→LUMO) and (HOMO→LUMO) configuration transitions. The solvent decrease coefficient of the (HOMO-2→LUMO) configuration from 0.939 to 0.751, while the additional (HOMO → LUMO) configuration appears with a coefficient 0.584. The (HOMO → LUMO) configuration of the CT state remains almost unchanged by the solvent (0.967 for vacuum and 0.942 for cyclohexane), but the effect on the orbital shape is more pronounced: in the solvent, HOMO of TTF is spread over the TTF and dibenzo-BODIPY moieties which decreases the dipole moment of the excited state. Due to influence of the solvent, the lowest exciton states are mixed with the CT state which reduces their energies and increases the dipole moments (Tables 1 and 2).

The ‘Chain’ molecule does not have a gate which can be considered a part of the internal subsystem. The rate of radiative recombination is ca. 10^7 – 10^8 s^{-1} for all gates. The (○●○) state corresponding to the excited intermediate

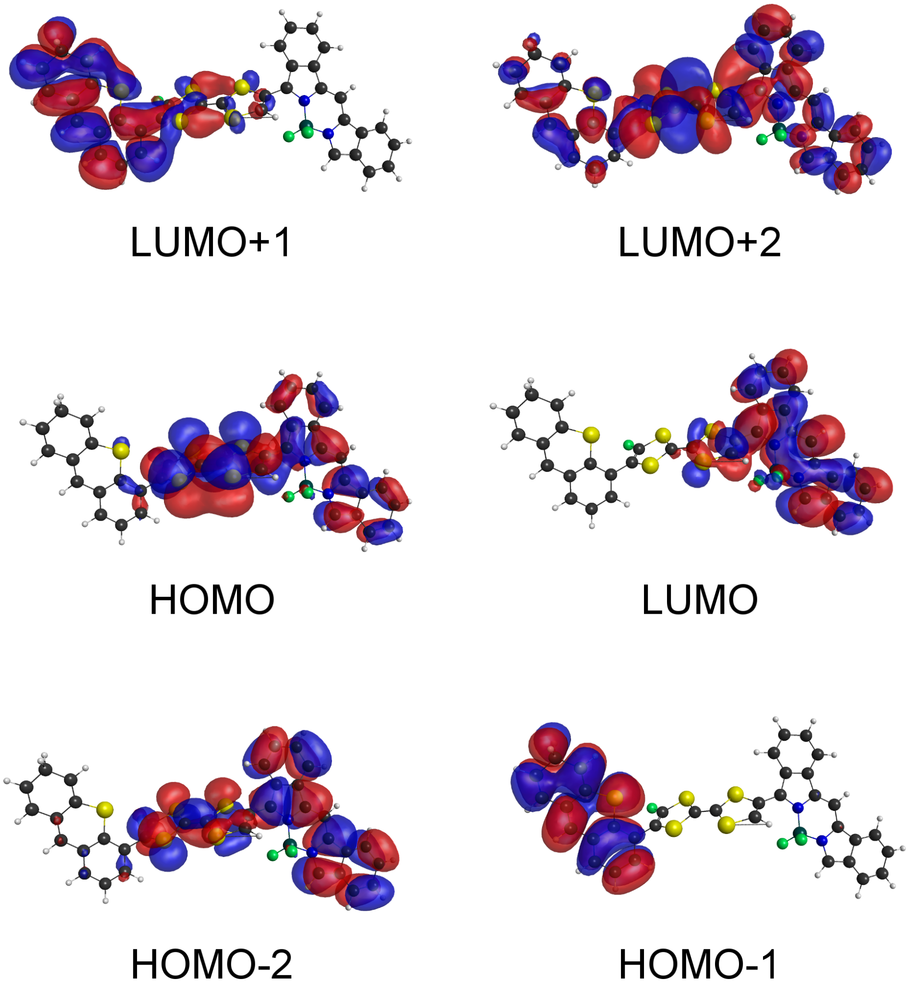

Figure 3: Frontier orbitals of the ‘Chain’ molecule.

Table 2: Energies and dipole moments of electronic states for the ‘Chain’ molecule in *cyclohexane*. The energy of the ground state in vacuum is chosen as the zero level.

State	Configuration	Energy (eV)		Moment (D)
		Cyclohexane	Vacuum	
e1	●−○−○	1.718	2.901	7.035
e2	○−●−○	1.470	2.551	3.562
e3	○−○−●	1.090	2.554	7.627
e4	○−⊕−⊖	0.817	2.029	4.755
e0	○−○−○	-1.119	0.0	3.340

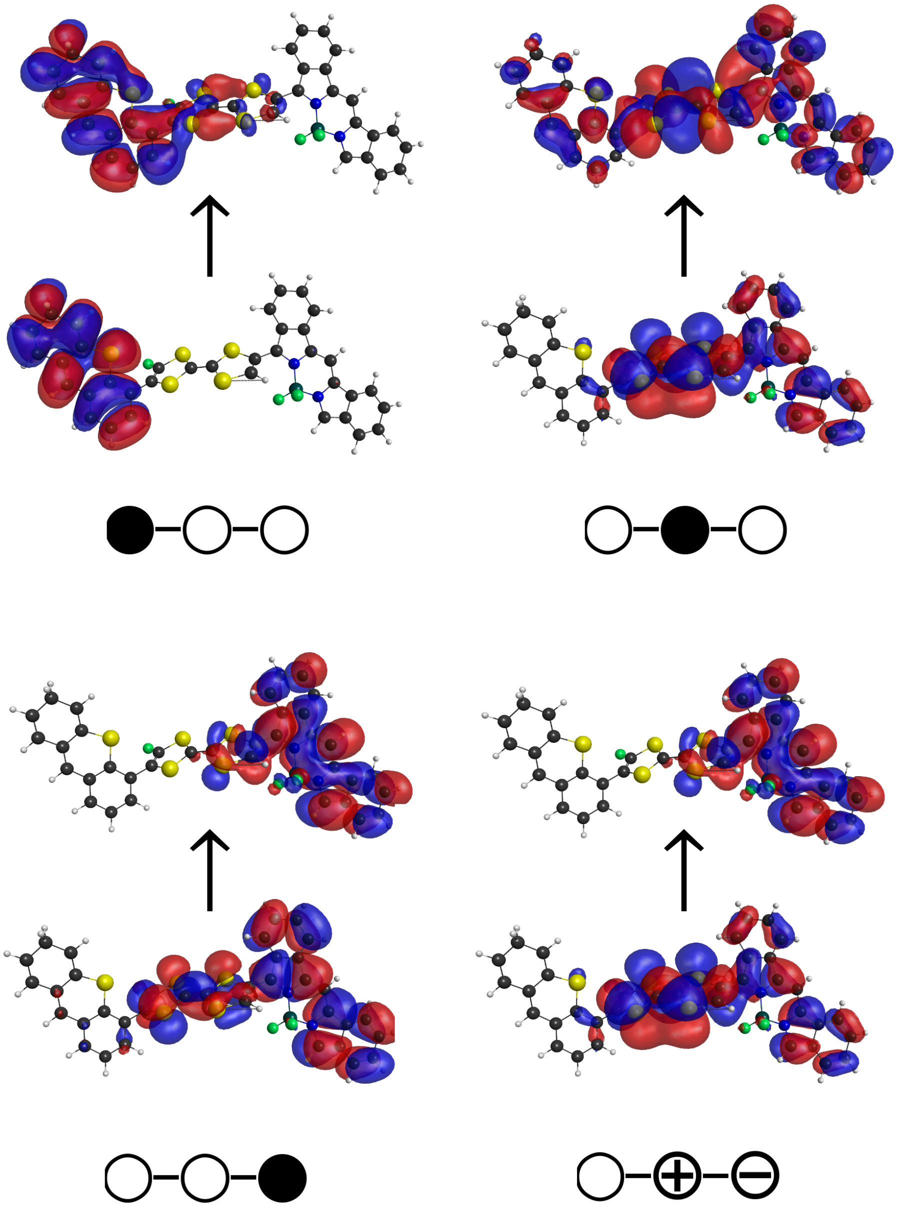

Figure 4: The dominating configurations of excited states for the ‘Chain’ molecule.

Table 3: Transitions between the states of ‘Chain’ in *vacuum*. E_{if}^{ver} is the energy of the vertical transition, E_{if} is the energy of the adiabatic transition, Ξ is the parameter of distortion, k_{IC} is the non-adiabatic transfer rate, k_{Rad} is the radiative transfer rate, $FWHM$ is the full width at half maximum for the density of states of the transition.

Transition	Initial	Final	$E_{if}^{ver}(eV)$	$E_{if}(eV)$	$\Xi(\%)$	$k_{IC}(s^{-1})$	$k_{Rad}(s^{-1})$	$FWHM(eV)$
$e1 \rightarrow e2$	●−○−○	○−●−○	0.27	0.4	56.7	Non.conv.	$3.1 \cdot 10^{2}$	0.009
$e1 \rightarrow e3$	●−○−○	○−○−●	0.09	0.43	58.6	0.0	$1.1 \cdot 10^{2}$	0.018
$e1 \rightarrow e4$	●−○−○	○−⊕−⊖	0.35	0.89	46.9	$8.5 \cdot 10^{10}$	$7.5 \cdot 10^{3}$	0.014
$e2 \rightarrow e3$	○−●−○	○−○−●	0.21	0.03	36.6	$5.7 \cdot 10^{13}$	$4.6 \cdot 10^{3}$	0.014
$e2 \rightarrow e4$	○−●−○	○−⊕−⊖	0.21	0.5	44.1	$3.6 \cdot 10^{14}$	$1.1 \cdot 10^{4}$	0.012
$e3 \rightarrow e4$	○−○−●	○−⊕−⊖	0.35	0.47	66.6	$2.3 \cdot 10^{14}$	$9.5 \cdot 10^{5}$	0.004
$e1 \rightarrow e0$	●−○−○	○−○−○	2.54	2.9	69.1	$3.4 \cdot 10^{4}$	$4.6 \cdot 10^{7}$	0.019
$e2 \rightarrow e0$	○−●−○	○−○−○	2.34	2.5	47.1	$3.5 \cdot 10^{5}$	$1.9 \cdot 10^{7}$	0.014
$e3 \rightarrow e0$	○−○−●	○−○−○	2.39	2.47	2.9	0.0	$1.5 \cdot 10^{8}$	0.005
$e4 \rightarrow e0$	○−⊕−⊖	○−○−○	1.84	2.0	55.4	$9.0 \cdot 10^{10}$	$5.9 \cdot 10^{7}$	0.007

YES-gate should be darker than the neighboring states but it has the same recombination rate. Due to distortion of molecular geometry, the (σ^*)-orbital of TTF is mixed with the (π^*)-orbital of the neighboring units, both for the system in vacuum and cyclohexane. Because of that, the (○●○) state becomes bright making TTF unfit for the internal subsystem.

The mixing of states influences not only recombination rates, but also exciton movement. The rates of radiative transitions between two excited states are of order $10^2 - 10^5$ s^{-1} in vacuum and $0 - 10^6$ s^{-1} in cyclohexane. The value of a rate decreases as the energy gap between the initial and final states increases. Among above mentioned transitions, radiative decay of an exciton into a hole and an electron has the highest rate which is around $10^5 - 10^6$ s^{-1}. The radiative transition between excited states caused by delocalization of state orbiatals. The delocalization leads to overlapping between neighboring states, which makes radiative transition between them allowed. This produces the undesirable result that exciton movement is accompanied by emitting of light, while the exciton should move non-radiatively.

Despite the drawbacks described above, the ‘Chain’ has an advantage related to a narrow absorption band in vacuum. The FWHM parameters have the values of 0.019, 0.014, 0.005 and 0.007 eV for the (●○○), (○●○), (○○●) and (○⊕⊖) states, respectively (Tables 3). The differences between the (●○○) state and the (○●○), (○○●), (○⊕⊖) states are of 0.4, 0.43 and 0.89 eV (Table 3). The molecule has to be irradiated with 305-309 nm light to be excited to the (●○○) state. The state of (○●○) has an excitation window of 340-343 nm, while the (○○●) and (○⊕⊖) states have windows of 345-346 nm and 396-399 nm, respectively. All these states have narrow spectral bands, which is why one can excite each state selectively. This allows generating an exciton precisely at the 3H-thioxanthene moiety.

Cyclohexane broadens bandwidths as shown in Table 4. For the molecule in solvent, they lie in the range of 382-437 nm for the (●○○) state, 444-479 nm for the (○●○) state, 533-561 nm for the (○○●) state, 511-639 nm for the (○⊕⊖) state. Despite this, the bands of (○●○) and (○○●) states do not overlap due to shifting of their energies. However, the band of the (○●○) becomes closer to the (●○○) band. The border between them is very arbitrary. If the oscillator strength of the (○●○) state was several orders of magnitude lower than the (●○○) and (○○●) states, we could neglect the excitation of the last one. But since they have similar brightness, selective excitation is difficult. To improve selectivity, one should shift to shorter wavelength sacrificing efficiency of excitation.

The ‘Chain’ molecule does not meet the requirements of the Franck–Condon approximation (see Introduction section for details) because its geometry becomes distorted as a result of transition. Not only does the TTF moiety change from a boat-like shape to planar, but also all the moieties rotate as a result of exciton passing. Since the Ξ parameter is significantly higher than the threshold value of 10% (Table 3 and 4), the validity of non-adiabatic rates can not be assured. In the general case, the non-radiative rates obey the energy gap law. The obtained rates break this law in both environments which manifests as greatly overestimated relaxation rates. All these facts further reduce the confidence reliability of the obtained non-adiabatic rates.

4.2 Line

The low excited states of the ‘Line’ molecule are ordered in the same way as the states of ‘Chain’: three exciton states form an energy ladder, and the CT state lies beneath them. However, the latter state has a higher energy compared to the analogous state in the ‘Chain’. Cyclohexane further increases the energy of this state, leading to the (○○●) and (○⊕⊖) states changing order. In contrast to the ‘Chain’, the exciton state does not mix with the CT state in the solvent. This is reflected in the dipole moments of these states which are approximately the same in both environments (Table 5 and 6).

Table 4: Transitions between the states of 'Chain' in *cyclohexane*. E_{if}^{ver} is the energy of the vertical transition, E_{if} is the energy of the adiabatic transition, E_{λ}^{Slow} is the solvation energy in the slow limit, E_{λ}^{Fast} is the solvation energy in the fast limit, Ξ is the parameter of distortion, k_{IC} is the non-adiabatic transfer rate, k_{Rad} is the radiative transfer rate, $FWHM$ is the full width at half maximum for the density of states of the transition.

Transition	Initial	Final	E_{if}^{Ver} (eV)	E_{if} (eV)	E_{λ}^{Slow} (eV)	E_{λ}^{Fast} (eV)	$\Xi(\%)$	$k_{IC}(s^{-1})$	$k_{Rad}(s^{-1})$	$FWHM$ (eV)
$e1 \to e2$	●–○–○	○–●–○	0.35	0.25	−0.1	−0.01	58.4	$1.1 \cdot 10^5$	0.0	0.081
$e1 \to e3$	●–○–○	○–○–●	0.16	0.63	0.28	0.38	59.7	~ 0	~ 0	0.130
$e1 \to e4$	●–○–○	○–⊕–⊖	0.37	0.90	0.03	−0.002	66.2	0	0	0.078
$e2 \to e4$	○–●–○	○–⊕–⊖	0.45	0.65	0.13	0.08	89.6	~ 0	$1.2 \cdot 10^6$	0.110
$e2 \to e3$	○–●–○	○–○–●	0.05	0.38	0.38	0.29	64.0	$1.1 \cdot 10^{16}$ (*)	$2.5 \cdot 10^3$	0.072
$e3 \to e4$	○–○–●	○–⊕–⊖	0.19	0.27	−0.25	−0.34	96.5	~ 0	$1.8 \cdot 10^5$	0.160
$e1 \to e0$	●–○–○	○–○–○	2.47	2.84	−0.06	0.006	72.4	$2.3 \cdot 10^9$	$7.4 \cdot 10^7$	0.136
$e2 \to e0$	○–●–○	○–○–○	2.46	2.59	0.04	0.006	61.2	$1.7 \cdot 10^7$	$2.5 \cdot 10^7$	0.068
$e3 \to e0$	○–○–●	○–○–○	2.26	2.21	−0.35	−0.04	55.0	$3.3 \cdot 10^8$	$8.5 \cdot 10^7$	0.039
$e4 \to e0$	○–⊕–⊖	○–○–○	1.80	1.94	−0.09	0.02	91.8	~ 0	$1.3 \cdot 10^8$	0.162

(*) The transition is beyond the limits of applicability of the theory.

Table 5: Energies and dipole moments of electronic states for the 'Line' molecule in *vacuum*. The energy of the ground state is chosen as the zero level.

State	Configuration	Energy (eV)	Moment
e1	●–○–○	2.831	4.902
e2	○–●–○	2.763	4.468
e3	○–○–●	2.739	4.165
e4	○–⊕–⊖	2.575	31.311
e0	○–○–○	0.0	4.024

Both molecules are formed by the same moieties but the ways of connecting them are different. More rigid structure help preventing the mixing of exciton states with the CT states.

The connection type used in the 'Line' prevents the (σ^*)-orbitals of TTF being mixed with (π^*)-orbitals of the neighboring moieties. Mixing takes place in 'Chain' because the TTF unit can be rotated relatively to the rest of the molecule. The rigid structure decreases the rate of radiative recombination to $3.3 \cdot 10^4$ s^{-1} for the TTF fragment (Table 7). For other states, radiative rates stay in the range of $10^7 - 10^9$ s^{-1}. Radiative transitions between excited states are almost forbidden. The recombination rates of the terminal gates are the highest among all radiative rates. The characteristic rates of the 'Line' molecule meet the requirements which are set for the desired system. The central gate can be viewed as a separate internal system which almost does not interact with light. Thus, an exciton can move through the molecule without absorption and fluorescence. It follows that an MLS should have a rigid structure in which units cannot move relative to each other.

Bandwidths of the absorption bands are higher for the 'Line' molecule according to FWHM values (Tables 7 and 8). In vacuum, the bandwidth is 404-422 nm for the (●○○) state, 391-449 nm for the (○●○) state, 430-453 nm for the (○○●) state, 426-481 nm for the (○⊕⊖) state. In cyclohexane the bandwidth is 412-429 nm for the (●○○) state, 386-444 nm for the (○●○) state, 413-468 nm for the (○○●) state, 509-510 nm for the (○⊕⊖) state. The bands overlap with each

Table 6: Energies and dipole moments of electronic states for the 'Line' molecule in *cyclohexane*. The energy of the ground state in vacuum is chosen as the zero level.

State	Configuration	Energy (eV) Cyclohexane	 Vacuum	Moment
e1	●–○–○	1.771	2.947	6.028
e2	○–●–○	1.671	2.762	5.010
e3	○–⊕–⊖	1.528	2.585	34.683
e4	○–○–●	1.311	2.738	5.895
e0	○–○–○	-1.122	0.0	4.557

Table 7: Transitions between the states of ‘Line’ in *vacuum*. E_{if}^{ver} is the energy of the vertical transition, E_{if} is the energy of the adiabatic transition, Ξ is the parameter of distortion, k_{IC} is the non-adiabatic transfer rate, k_{Rad} is the radiative transfer rate, $FWHM$ is the full width at half maximum for the density of states of the transition.

Transition	Initial	Final	$E_{if}^{Ver}(eV)$	$E_{if}(eV)$	$\Xi(\%)$	$k_{IC}(s^{-1})$	$k_{Rad}(s^{-1})$	$FWHM(eV)$
$e1 \rightarrow e2$	●–○–○	○–●–○	0.30	0.18	27.6	$6.3 \cdot 10^{12}$	0.0	0.104
$e1 \rightarrow e3$	●–○–○	○–○–●	0.10	0.20	3.1	$5.1 \cdot 10^{15}$ (*)	$1.2 \cdot 10^{3}$	0.027
$e1 \rightarrow e4$	●–○–○	○–⊕–⊖	0.03	0.46	26.8	$7.9 \cdot 10^{15}$ (*)	$2.7 \cdot 10^{2}$	0.079
$e2 \rightarrow e3$	○–●–○	○–○–●	0.24	0.02	43.4	$1.3 \cdot 10^{11}$	0.0	0.092
$e2 \rightarrow e4$	○–●–○	○–⊕–⊖	0.14	0.19	3.3	$2.0 \cdot 10^{14}$	0.0	0.026
$e3 \rightarrow e4$	○–○–●	○–⊕–⊖	0.0042	0.16	46.5	$7.1 \cdot 10^{16}$ (*)	0.0	0.067
$e1 \rightarrow e0$	●–○–○	○–○–○	2.54	2.94	28.3	$3.0 \cdot 10^{5}$	$4.8 \cdot 10^{8}$	0.042
$e2 \rightarrow e0$	○–●–○	○–○–○	2.70	2.76	64.7	$2.8 \cdot 10^{9}$	$3.3 \cdot 10^{4}$	0.137
$e3 \rightarrow e0$	○–○–●	○–○–○	2.70	2.74	60.9	$8.9 \cdot 10^{8}$	$5.9 \cdot 10^{8}$	0.047
$e4 \rightarrow e0$	○–⊕–⊖	○–○–○	2.35	2.58	64.7	$1.0 \cdot 10^{10}$	$3.7 \cdot 10^{7}$	0.111

(*) The transition is beyond the limits of applicability of the theory.

Table 8: Transitions between the states of ‘Line’ in *cyclohexane*. E_{if}^{ver} is the energy of the vertical transition, E_{if} is the energy of the adiabatic transition, E_{λ}^{Slow} is the solvation energy in the slow limit, E_{λ}^{Fast} is the solvation energy in the fast limit, Ξ is the parameter of distortion, k_{IC} is the non-adiabatic transfer rate, k_{Rad} is the radiative transfer rate, $FWHM$ is the full width at half maximum for the density of states of this transition.

Transition	Initial	Final	E_{if}^{Ver} (eV)	E_{if} (eV)	E_{λ}^{Slow} (eV)	E_{λ}^{Fast} (eV)	$\Xi(\%)$	$k_{IC}(s^{-1})$	$k_{Rad}(s^{-1})$	$FWHM$ (eV)
$e1 \rightarrow e2$	●–○–○	○–●–○	0.42	0.10	−0.08	−0.004	32.3	$2.7 \cdot 10^{10}$	0.0	0.114
$e1 \rightarrow e3$	●–○–○	○–⊕–⊖	0.19	0.24	−0.12	0.02	29.0	$7.1 \cdot 10^{11}$	$2.0 \cdot 10^{3}$	0.090
$e1 \rightarrow e4$	●–○–○	○–○–●	0.15	0.46	0.25	−0.01	20.6	$8.7 \cdot 10^{14}$ (*)	$3.7 \cdot 10^{2}$	0.040
$e2 \rightarrow e3$	○–●–○	○–⊕–⊖	0.19	0.14	−0.04	0.03	4.6	$1.1 \cdot 10^{14}$	0.0	0.025
$e2 \rightarrow e4$	○–●–○	○–○–●	0.10	0.36	0.34	0.01	64.5	$4.9 \cdot 10^{11}$	0.0	0.141
$e3 \rightarrow e4$	○–⊕–⊖	○–○–●	0.06	0.22	0.37	−0.009	73.8	$2.7 \cdot 10^{11}$	$1.3 \cdot 10^{3}$	0.118
$e1 \rightarrow e0$	●–○–○	○–○–○	2.62	2.89	−0.05	0.004	23.7	$8.8 \cdot 10^{5}$	$8.2 \cdot 10^{7}$	0.041
$e2 \rightarrow e0$	○–●–○	○–○–○	2.58	2.79	0.03	−0.002	67.7	$6.0 \cdot 10^{9}$	$3.1 \cdot 10^{4}$	0.142
$e3 \rightarrow e0$	○–⊕–⊖	○–○–○	2.45	2.65	0.07	−0.01	69.4	$1.1 \cdot 10^{10}$	$1.5 \cdot 10^{7}$	0.118
$e4 \rightarrow e0$	○–○–●	○–○–○	2.39	2.43	−0.3	−0.007	6.2	~ 0	$4.1 \cdot 10^{8}$	0.001

(*) The transition is beyond the limits of applicability of the theory.

other due to the low difference between the state energies. As can be seen, the main part of the (●○○) band overlaps with the (○●○) band which makes the oscillator strength of the former state higher by four orders of magnitude. This allows to regard the side excitation as a low-intensity one in comparison with the target excitation. Overlapping of (●○○) with (○○●) and (○⊕⊖) is more critical in this regard since they have the same intensity. One should avoid the spectral range where bands overlap and shift the band to shorter wavelengths. By doing so, one can improve the selectivity of excitation at a cost of decreasing its efficiency.

Despite the improved way of connection, the ‘Line’ molecule is not rigid enough because of the TTF moiety in the middle. The molecule is bent if the TTF unit is in the ground state and planar when an exciton passes through this fragment. Distortions are reflected in the values of Ξ (Tables 7 and 8) which exceed the threshold value of 10%. Thus, the Franck-Condon approximation cannot be applied to these transitions, and the obtained non-adiabatic rates cannot be considered reliable. As is the case with the ‘Chain’, the rates similarly do not follow the energy gap law, resulting in overestimated rates of exciton relaxation. The sum of these factors does not allow using these values for building a kinetic model.

4.3 S-line

For a system of molecular logic gates to work properly, energies of its exciton states should form a downward ladder so that the excitaton energy could flow through it unidirectionally. While this is the case for the ‘Chain’ and ‘Line’ molecules, one of their low-lying states was the CT state which can be viewed as parasitic. In the ‘S-line’ molecule, the excitonic ladder is broken since the energy of the (○○●) state is shifted upwards relative to other states (Table 9). An exciton cannot use the (○○●) state for generating the output signal due to this shifting. However, there is the (○⊕⊖) state which is bright and which, together with the rest excitonic states, forms a ladder. When an exciton is generated at the 3H-thioxanthene moiety producing the (●○○) state, it passes through the sequence of the (○●○) and (○⊕⊖) states.

Table 9: Energies and dipole moments of electronic states for the ‘S-line’ molecule in *vacuum*. The energy of the ground state is chosen as the zero level.

State	Configuration	Energy (eV)	Moment
e1	○−○−●	3.005	12.831
e2	●−○−○	2.952	6.686
e3	○−●−○	2.757	4.222
e4	○−⊕−⊖	2.408	20.156
e0	○−○−○	0.0	4.475

Table 10: Energies and dipole moments of electronic states for the ‘S-line’ molecule in *cyclohexane*. The energy of the ground state in vacuum is chosen as the zero level.

State	Configuration	Energy (eV)		Moment
		Cyclohexane	Vacuum	
e1	●−○−○	1.792	2.956	8.266
e2	○−○−●	1.781	3.021	19.325
e3	○−●−○	1.700	2.757	4.681
e4	○−⊕−⊖	1.202	2.428	15.633
e0	○−○−○	-1.080	0.0	5.013

The (○○●) state does not take part in the process because the exciton does not have enough energy to hop up to this state. For this reason, we will take into account only 4 states for the ‘S-line’ in vacuum. Cyclohexane moves the energy of the (○○●) state lower than the (●○○) energy so that this state starts contributing to excited-states kinetics of the ‘S-line’ (Table 10). Therefore, one needs to take into account 5 states of the molecule in cyclohexane

The ‘S-line’ molecule can be divided into the external and internal subsystems as well as the ‘Line’. The radiative recombination in the TTF unit is slower by three orders of magnitude comparing to recombinations in other moieties. Radiative transitions between excited states either are forbidden or proceed extremely slow. The only exception is the decay of an exciton into an electron-hole pair which is facilitated by cyclohexane environment (see the (●○○)→(○⊕⊖) transition in tables 11 and 12). Photokinetics in the ‘S-line’ in most aspects is no different from that of the ‘Line’.

In tables 11 and 12 given are the bandwidths of the ‘S-line’ in vacuum which are of 411-420 nm for the (●○○) state, 440-429 nm for the (○●○) state, 504-515 nm for the (○⊕⊖) state. In cyclohexane, these bandwidths become 422-432 nm for the (●○○) state, 427-434 nm for the (○○●) state, 436-446 nm for the (○●○) state, 534-544 nm for the (○⊕⊖) state. The bands corresponding to 3H-thioxanthene and dibenzo-BODIPY moieties almost coincide for the molecule in cyclohexane. Because of that, one cannot excite the receiving gate selectively without acting on the transmitting gate.

The ‘S-line’ is more rigid than other constructions: the units do not rotate with respect to each other and the TTF moiety remains planar in each state. Rigidity of the ‘S-line’ is clear according to the Ξ parameter (Tables 11 and 12) which does not exceed the threshold value of 10%. The only exceptions are transitions related to the CT state for which the Ξ parameter varies between $10-17\%$. Since the excess of the threshold is not large, we will consider all transitions satisfying the Franck-Condon approximation. The Bixon-Jortner-Plotnikov theory can be applied for calculating the rates of these transitions, which subsequently can be used for building a kinetic model of the ‘S-line’.

In contrast to the rates obtained for the ‘Chain’ and ‘Line’, the non-adiabatic rates for the ‘S-line’ obey the energy gap law: the lower the gap between the initial and final state, the faster the non-adiabatic transitions are between them. Tables 11 and 12 show that the rates of exciton hopping are higher than the relaxation rates by $6-10$ orders of magnitude. The exciton moves between moieties with the rate of $10^{11}-10^{14}$ s^{-1} while the rate of exciton decay into a charge-transfer state is around $10^{13}-10^{15}$ s^{-1}. Relaxation to the ground state, meanwhile, is as slow as 10^{5} s^{-1}. Summarizing the obtained data, an exciton moves through the molecule mainly via a non-adiabatic pathway, while the transition to the ground states occurs mainly through radiative channel.

4.4 Kinetics of the excited states

The ‘S-line’ molecule in vacuum has a strong parasitic channel between the highest exciton state (●○○) and the charge-transfer state (○⊕⊖). The non-adiabatic rate of this transition equals $1.9\cdot 10^{13}$ s^{-1} which is ten times higher than the transfer rate from (●○○) to (○●○). This means that after excitation, 90% of excitons go directly to the finish state while only 10% of them will transfer via the supposed channel. From the (○●○) state, an exciton can proceed in two

Table 11: Transitions between the states of the ‘S-line’ in *vacuum*. E_{if}^{ver} is the energy of the vertical transition, E_{if} is the energy of the adiabatic transition, Ξ is the parameter of distortion, k_{IC} is the non-adiabatic transfer rate, k_{Rad} is the radiative transfer rate, $FWHM$ is the full width at half maximum for the density of states of this transition.

Transition	Initial	Final	$E_{if}^{Ver}(eV)$	$E_{if}(eV)$	$\Xi(\%)$	$k_{IC}(s^{-1})$	$k_{Rad}(s^{-1})$	$FWHM(eV)$
$e2 \rightarrow e3$	●−○−○	○−●−○	0.29	0.19	7.0	$2.7 \cdot 10^{12}$	0.0	0.035
$e2 \rightarrow e4$	●−○−○	○−⊕−⊖	0.14	0.60	2.0	$1.9 \cdot 10^{13}$	$4.2 \cdot 10^{2}$	0.034
$e3 \rightarrow e4$	○−●−○	○−⊕−⊖	0.07	0.35	5.8	$1.1 \cdot 10^{15}$ (*)	0.0	0.004
$e2 \rightarrow e0$	●−○−○	○−○−○	2.65	2.95	7.4	$1.6 \cdot 10^{4}$	$3.5 \cdot 10^{7}$	0.022
$e3 \rightarrow e0$	○−●−○	○−○−○	2.55	2.76	8.0	2.81	$3.75 \cdot 10^{4}$	0.020
$e4 \rightarrow e0$	○−⊕−⊖	○−○−○	2.27	2.41	11.3	$1.2 \cdot 10^{3}$	$1.5 \cdot 10^{8}$	0.017

(*) The transition is beyond the limits of applicability of the theory.

Table 12: Transitions between the states of the ‘S-line’ in *cyclohexane*. E_{if}^{ver} is the energy of the vertical transition, E_{if} is the energy of the adiabatic transition, E_{λ}^{Slow} is the solvation energy in the slow limit, E_{λ}^{Fast} is the solvation energy in the fast limit, Ξ is the parameter of distortion, k_{IC} is the non-adiabatic transfer rate, k_{Rad} is the radiative transfer rate, $FWHM$ is the full width at half maximum for the density of states of this transition.

Transition	Initial	Final	E_{if}^{Ver} (eV)	E_{if} (eV)	E_{λ}^{Slow} (eV)	E_{λ}^{Fast} (eV)	$\Xi(\%)$	$k_{IC}(s^{-1})$	$k_{Rad}(s^{-1})$	$FWHM$ (eV)
$e1 \rightarrow e2$	●−○−○	○−○−●	0.39	0.01	0.08	0.07	7.7	$1.2 \cdot 10^{12}$	$2.0 \cdot 10^{3}$	0.031
$e1 \rightarrow e3$	●−○−○	○−●−○	0.41	0.09	−0.11	−0.002	4.2	$4.5 \cdot 10^{11}$	0.0	0.037
$e1 \rightarrow e4$	●−○−○	○−⊕−⊖	0.20	0.59	0.06	−0.007	2.0	$1.8 \cdot 10^{13}$	0.0	0.032
$e2 \rightarrow e3$	○−○−●	○−●−○	0.12	0.08	−0.18	−0.01	12.8	$2.2 \cdot 10^{14}$	0.0	0.009
$e2 \rightarrow e4$	○−○−●	○−⊕−⊖	0.54	0.58	−0.01	0.02	0.3	$2.1 \cdot 10^{13}$	$5.1 \cdot 10^{6}$	0.003
$e3 \rightarrow e4$	○−●−○	○−⊕−⊖	0.23	0.50	0.17	0.03	5.4	$3.9 \cdot 10^{13}$	0.0	0.085
$e1 \rightarrow e0$	●−○−○	○−○−○	2.55	2.87	−0.08	0.002	4.0	$1.9 \cdot 10^{5}$	$7.3 \cdot 10^{7}$	0.022
$e2 \rightarrow e0$	○−○−●	○−○−○	2.77	2.86	−0.16	−0.01	10.2	~ 0	$1.3 \cdot 10^{8}$	0.015
$e3 \rightarrow e0$	○−●−○	○−○−○	2.58	2.78	0.02	−0.004	7.9	1.75	$4.3 \cdot 10^{4}$	0.021
$e4 \rightarrow e0$	○−⊕−⊖	○−○−○	2.20	2.28	−0.15	−0.009	17.1	$5.2 \cdot 10^{2}$	$2.3 \cdot 10^{8}$	0.014

ways: de-excitation (●○○)→(○○○) and transfer (●○○)→(○⊕⊖). The first way is very slow ($3.75 \cdot 10^{4}$ s^{-1}) while the second has a very large rate of ($1.1 \cdot 10^{15}$ s^{-1}) . Thus, an exciton hops to the finish state practically without losses. Since optical de-excitation of the (○⊕⊖) state is slower than any channel leading to this state by several orders of magnitude, an exciton stays there for 100 ns. This feature can be clearly seen in 5: exciton directly transfers from (●○○) to (○⊕⊖) in 100 fs without stopping in the (○●○) state first.

A similar picture can be seen for the ‘S-line’ molecule in cyclohexane (Fig. 6). The solvent decreases the energy of the (○○●) state and makes it a part of the workspace. Now, the exciton has three ways: e1→e4, e1→e3→e4 and e1→e2→e3→e4. Two of these ways are parasitic, one connecting the start and the finish states and the other forming a shortcut. The presence of a loop leads to a very small increase of the population of the (○●○) state but it practically does not change the general kinetics due to a very high rate of the (○●○)→(○⊕⊖) transition. In both cases, vacuum and cyclohexane, the main problem is the very fast transition between nonadjacent fragments which leads to parasitic lines in a logic scheme.

The non-adiabatic transfer rate depends on the overlap of orbitals of the initial and final states, the adiabatic and vertical transition energies. The overlap and the vertical energy affects the coupling while the adiabatic energy determines the density of states in the transition window. It was expected that the rates of the (●○○)→(○⊕⊖) and (●○○)→(○○●) transitions would be lower than the rate of the (●○○)→(○●○) transition since the overlap between the initial and final states is lower for the first and second transitions than for the third one. They also should have a larger gap between adiabatic energies which leads to lower density of states. Both these factors decrease the transition rate but the (●○○)→(○⊕⊖) and (●○○)→(○○●) transitions actually have higher rate constants.

It is unlikely that the symmetry type influences the transfer rate. In this research, we consider specific non-adiabatic transitions between states with different characters: $\pi\sigma^*$-type and $\pi\pi^*$-type. Since the (●○○)→(○●○) transition is a transition with the change of symmetry and the (●○○)→(○○●) and (●○○)→(○⊕⊖) transition occurs without symmetry change, one can decide that symmetry type can have an effect on the transfer rate. On the other side, the (○○●)→(○●○) and (○●○)→(○⊕⊖) transitions also have large rates although they occur with the change of the symmetry type. This means that the character of the initial and finial states, $\pi\sigma^*$-type or $\pi\pi^*$-type, is not that relevant.

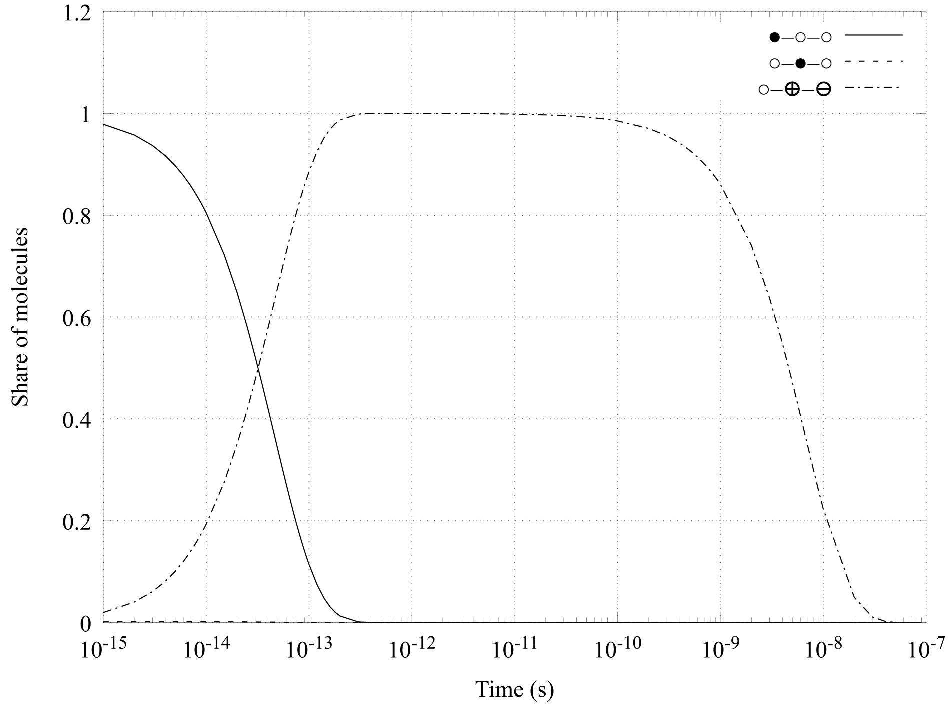

Figure 5: Kinetics of excited states for the ‘S-line’ molecule in vacuum.

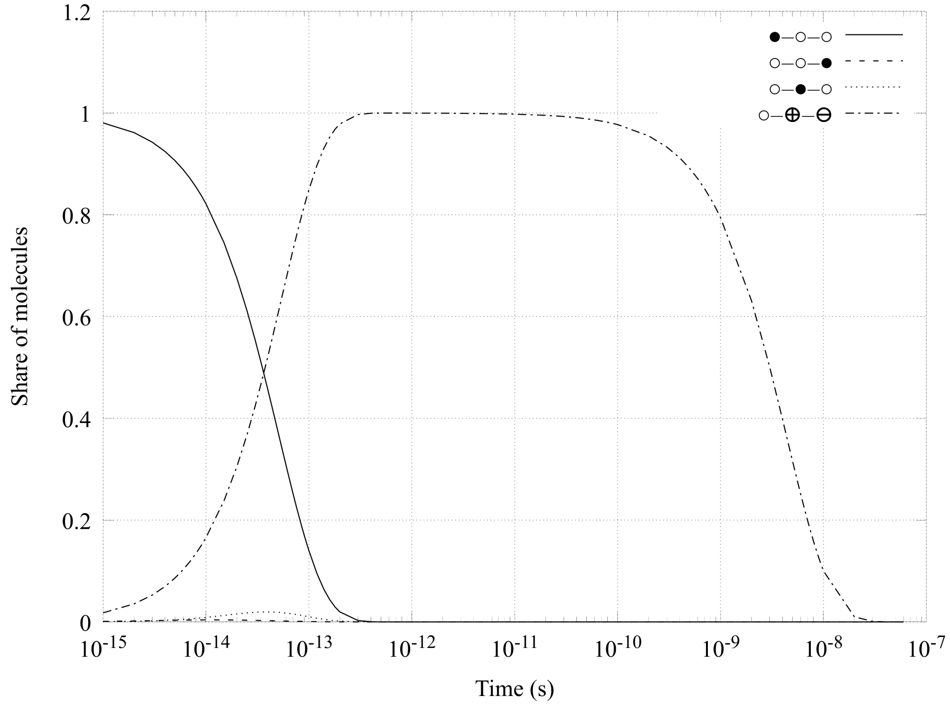

Figure 6: Kinetics of excited states for the ‘S-line’ molecule in vacuum on the assumption that the (●○○) is excited selectively at the start.

It seems that the adiabatic energy is a more important factor than the vertical energy because the density of states directly depends on this parameter. The non-adiabatic coupling only linearly depends on the vertical energy. The vertical transition energy is the difference between the energies of the initial and final states in the same geometries, in our case – in the initial geometry. Meanwhile, the adiabatic transition energy is the difference between the energies calculated in equilibrium geometries of each state. However, the rate constant correlates more strongly with the vertical energy than with the adiabatic one. If one takes constants for transitions between excited states as a statisctical sample, the coefficient of correlation is -0.705 between E_{if}^{Ver} and $\log k_{IC}$ while the coefficient is 0.369 between E_{if} and $\log k_{IC}$. If one adds high energy transitions to the sample, the correlation coefficients are -0.966 and -0.936 for vertical and adiabatic energies, respectively. It is apparent that the vertical energy has a much greater influence on the non-adiabatic rate in comparison to other parameters.

The parasitic channel is not the only problem which can be caused by two closely spaced levels. If they both are bright and their absorption bands overlap, one can not excite one state separately from another. The (●○○) and (○○●) states overlap for the ‘S-line’ solvated in cyclohexane. Assume that all molecules in a system are in the ground state in the initial moment of time. Light irradiation excites some of the molecules into the (●○○) state, and the other part into the (○○●) state. We assume that they are excited in equal shares resulting in kinetics shown in Fig. 7. The (○⊕⊖) state reaches a maximum faster but this is caused by dibenzo-BODIPY being excited from the beginning.

Heat dissipation is another important characteristic of an MLS. The ‘S-line’ dissipates 0.59 eV of energy in the environment after exciton is passed. Let us assume a 0.01M solution of the ‘S-line’ molecules in cyclohexane and a laser beam being able to excite all molecules into the (●○○) state at once. Under such conditions, they would heat the solvent by 0.4 K per cycle. As can be seen from Fig. 5, an interval of 16 ns is enough for an exciton to pass though the molecule. If a delay between laser pulses is 16 ns, cyclohexane will be heated to the boiling point in 2.4 μs. After this moment, the operation should be stopped until the solvent cools down. Such scale of heat dissipation seems large but let us put it into perspective and compare this system with a conventional CPU. As an example, take Core i7-3770K (22 nm) [47], which has a frequency of 3.5-3.9 GHz and thermal design power (TDP) of 77 W. The CPU contains 1.4 billion transistors [48]. A logic gate can include several transistors but we will consider an MLG as one transistor for simplicity. For $4 \cdot 10^9$ cycles, the system of 1.4 billion MLGs releases 0.54 J of heat per 64 s while the conventional CPU dissipates 77 J per 1 s. The MLG releases less energy by two orders of magnitude, albeit in an increased operation time.

There are two main issues that can be encountered after dividing an MLS into two subsystems. Firstly, states of these subsystems can be mixed in flexible molecules. When moieties rotate with respect to each other, ($\pi\sigma^*$)-states mix with ($\pi\pi^*$)-states. This causes them to become bright and unable to play the role of gates of the internal subsystem. Secondly, the parasitic channels can form between closely lying states. If the gap between states is less than FWHM of the transition between them, they can be considered as resonance states. Moreover, the energy of vertical transition is of greater importance compared to the energy of adiabatic transition. The rate of non-adiabatic transfer between them will be maximal at a certain value of non-adiabatic coupling. This feature is useful if one needs to accelerate the transfer between moieties. However, if two unlinked closely spaced gates have such states, the system has a parasitic line. Therefore, an MLS should have a rigid structure which does not deform upon exciton movement, and the system must not have parasitic resonance between closely spaced gates.

5 Conclusion

In this work we attempted to divide a molecular logic system into two subsystems (external and internal) and studied signal exchange between them. The external subsystem includes the input and output gates which are located at different sides of the molecule. Both types of gates interact with light, receiving and transmitting external signals. The external subsystem plays the role of an interface between the MLS and outside devices while the internal subsystem processes a signal. It is based on using dark states which do not interact with light. This prevents possible failures caused by light noise and long-term radiative interaction. To ensure such division, excited states of two types are used: ($\pi\pi^*$)-states for the external subsystem and ($\pi\sigma^*$)-states for the internal one. The objective was to show that excitation can move through such a system and pass through the boundary between the subsystems belonging to different types.

We considered a very simple system of this type which consisted of a receiver, a YES-gate and a transmitter. As a model system, a molecule consisting of 3H-thioxanthene, TTF and dibenzo-BODIPY units was taken, in which each moiety corresponds to a gate of the system. Two terminal moieties constituted external subsystem while the central part plays the role of a YES-gate. Kinetic rates of transition between electronic states were calculated for various linkage types of units in the molecule in vacuum and cyclohexane. The rates were obtained within the frame of the Bixon-Jortner-Plotnikov theory.

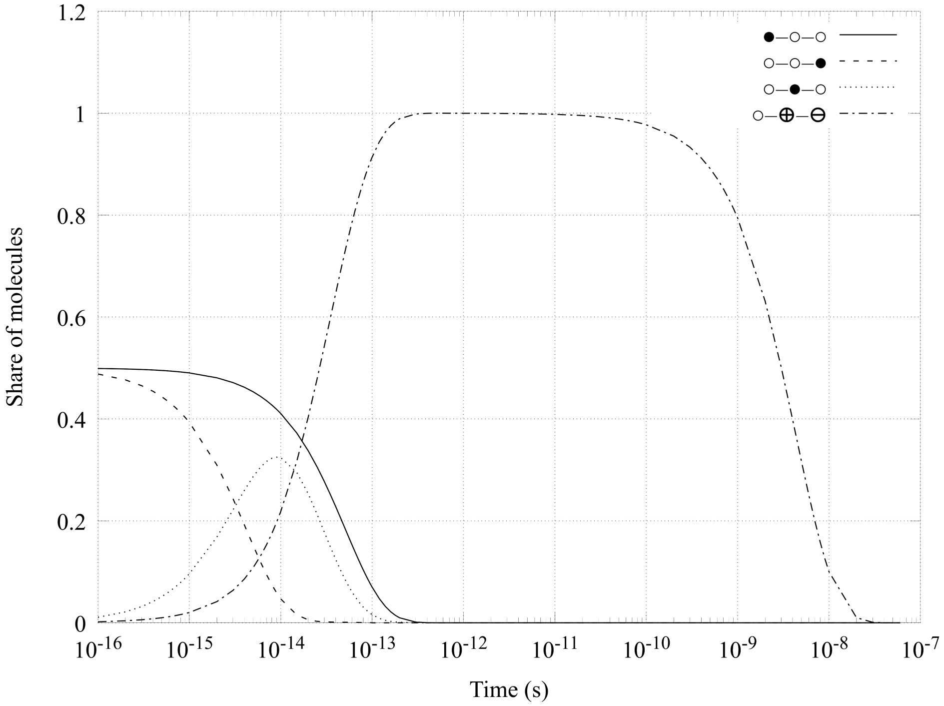

Figure 7: Kinetics of excited states for the ‘S-line’ molecule in vacuum on the assumption that the (●○○) and (○○●) states are excited with an equal probability.

As a result, it was found that the realization of the desired MLS is possible. In such a system, an exciton moves via the non-adiabatic channel which allows it to hop between the gates with different types of orbital symmetry. The dark character of the gates in the inner part protects the exciton from premature recombination. The bright states are reserved only for special moieties which use radiative transitions for absorption and fluorescence. The gradient of energy between the gates ensures a directional movement of an exciton within the system itself. The work of the MLS is based on the fact that non-adiabatic transfer rate decreases with increasing transfer energy, but the rates of radiative transitions increase as the energy multiplied by oscillator strength squared. It turns out that the radiative recombination is the main path from an excited to the ground state, while the transfer between excited states occurs non-radiatively.

To be separable into two subsystems, an MLS has to have a rigid structure which maintains its geometry during exciton movement to prevents mixing of ($\pi\pi^*$) and ($\pi\sigma^*$) states. In the system, the LUMO of a gate should not be close to HOMO of the next gate to avoid the formation of a charge transfer (CT) state in the excitonic channel. The CT states are a problem for MLSs based on excitonic signals due to their ability to mix with operational exciton states changing their energies and other properties. Furthermore, two neighboring gates must not have two states with close energies because they can form a parasitic line in the logic circuit. These guidelines were obtained from an analysis of an oversimplified MLS but it does not lessen their importance. These findings can be applied to complex MLSs too, allowing one to use them as rules for design of molecular logic systems.

Conflicts of interest

There are no conflicts to declare.

Acknowledgements

The study was carried out as a part of the state project ’The structure and dynamics of atomic-molecular system’ and also was supported (partially) by the Ministry of Science and Higher Education of the Russian Federation in the framework of state task FSMR-2023-0002 (DFT and TD-DFT calculations)

References

[1] P. Ball. Chemistry meets computing. *Nature*, 406:118–120, 2000.

[2] R. Guliyev, S. Ozturk, Z. Kostereli, and E. U. Akkaya. From virtual to physical: integration of chemical logic gates. *Angew. Chem*, 123:10000–10005, 2011.

[3] U. Pischel, J. Andréasson, D. Gust, and V. F. Pais. Information processing with molecules—quo vadis? *ChemPhysChem*, 14:28–46, 2013.

[4] Madhuprasad, M. P. Bhat, H. Jung, D. Losic, and M. D Kurkuri. Anion sensors as logic gates: a close encounter? *Chem. Eur. J.*, 22:6148–6178, 2016.

[5] M. F. Budyka. Molecular switches and logic gates for information processing, the bottom-up strategy: from silicon to carbon, from molecules to supermolecules. *Russ. Chem. Rev.*, 86:181, 2017.

[6] L. Liu, P. Liu, L. Ga, and J Ai. Advances in applications of molecular logic gates. *ACS omega*, 6:30189–30204, 2021.

[7] T. Niazov, R. Baron, E. Katz, O. Lioubashevski, and I Willner. Concatenated logic gates using four coupled biocatalysts operating in series. *Proc. Natl. Acad. Sci.*, 103:17160–17163, 2006.

[8] T. Gupta and M. E. van der Boom. Redox-active monolayers as a versatile platform for integrating boolean logic gates. *Angew. Chem., Int. Ed. Engl.*, 47:5322–5326, 2008.

[9] T. Gupta and M. E. van der Boom. Chemical communication between metal-complex-based monolayers. *Angew. Chem., Int. Ed. Engl.*, 12:2260–2262, 2008.

[10] S. Silvi, E. C. Constable, C. E. Housecroft, J. E. Beves, E. L. Dunphy, M. Tomasulo, F. M. Raymo, and A Credi. All-optical integrated logic operations based on chemical communication between molecular switches. *Chem. Eur. J.*, 15:178–185, 2009.

[11] S. Speiser. Prospects of luminescence based molecular scale logic gates and logic circuits. *J. Lumin.*, 169:458–465, 2016.

[12] J. Andréasson and U. Pischel. Smart molecules at work—mimicking advanced logic operations. *Chem. Soc. Rev.*, 39:174–188, 2010.

[13] S. Erbas-Cakmak, S. Kolemen, A. C. Sedgwick, T. Gunnlaugsson, T. D. James, J. Yoon, and E. U. Akkaya. Molecular logic gates: the past, present and future. *Chem. Soc. Rev.*, 47:2228–2248, 2018.

[14] S. Erbas-Cakmak and E. U. Akkaya. Cascading of molecular logic gates for advanced functions: A self-reporting, activatable photosensitizer. *Angew. Chem.*, 125:11574–11578, 2013.

[15] H. Jiang, M. D. Riedel, and K. K. Parhi. Digital logic with molecular reactions. *2013 IEEE/ACM International Conference on Computer-Aided Design (ICCAD*, pages 721–727, 2013.

[16] A. P. de Silva, S. Uchiyama, T. P. Vance, and B. Wannalerse. A supramolecular chemistry basis for molecular logic and computation. *Coord. Chem. Rev.*, 251:1623–1632, 2007.

[17] S. Speiser. Photophysics and mechanisms of intramolecular electronic energy transfer in bichromophoric molecular systems: Solution and supersonic jet studies. *Chem. Rev*, 96:1953–1976, 1996.

[18] R. W. Wagner and J. S. A Lindsey. A molecular photonic wire. *J. Am. Chem. Soc.*, 116:9759–9760, 1994.

[19] R. W. Wagner, J. S. Lindsey, J. Seth, V. Palaniappan, and D. F. Bocian. Molecular optoelectronic gates. *J. Am. Chem. Soc.*, 118:3996–3997, 1996.

[20] A. Ambroise, C. Kirmaier, R. W. Wagner, R. S. Loewe, D. F. Bocian, D. Holten, and J. S. Lindsey. Weakly coupled molecular photonic wires: synthesis and excited-state energy-transfer dynamics. *J. Org. Chem.*, 67:3811–3826, 2002.

[21] E. T. Ecik, A. Atilgan, R. Guliyev, T. B. Uyar, A. Gumus, and E. U. Akkaya. Modular logic gates: cascading independent logic gates via metal ion signals. *Dalton Trans.*, 43:67–70, 2014.

[22] F. Remacle, Speiser S., and R. D. Levine. Intermolecular and intramolecular logic gates. *J. Phys. Chem. B*, 105:5589–5591, 2001.

[23] S. D. Straight, J. Andréasson, G. Kodis, S. Bandyopadhyay, R. H. Mitchell, T. Moore, A. Moore, and D. Guest. Molecular and and inhibit gates based on control of porphyrin fluorescence by photochromes. *J. Am. Chem. Soc*, 127:9403–9409, 2005.

[24] K. L. Kompa and R. D. Levine. A molecular logic gate. *Proc. Natl. Acad. Sci.*, 98:410–414, 2001.

[25] O. Kuznetz, D. Davis, H. Salman, Y. Eichen, and S. Speiser. Intramolecula electronic energy transfer in rhodamine-azulene bichromphoric molecule. *J. Photochem*, 191:176–181, 2007.

[26] O. Kuznetz, H. Salman, N. Shakkour, Y. Eichen, and S. Speiser. The azulene–rhodamine all optical full adder. *Mol. Phys.*, 106:531–535, 2008.

[27] O. Kuznetz, H. Salman, Y. Eichen, F. Remacle, R. D. Levine, and S. Speiser. All optical full adder based on intramolecular electronic energy transfer in the rhodamine-azulene bichromophoric system. *J. Phys. Chem*, 112:15880–15885, 2008.

[28] R. J. Hudson, T. S. C. MacDonald, J. H. Cole, T. W. Schmidt, T. A. Smith, and D. R. McCamey. A framework for multiexcitonic logic. *Nat. Rev. Chem.*, 8:136–151, 2024.

[29] A. I. Martynov, A. S. Belov, and V. K. Nevolin. The non-adiabatic exciton transfer in tetrathiafulvalene chains: a theoretical study of signal transmission in a molecular logic system. *Phys. Chem. Chem. Phys.*, 22:25243–25254, 2020.

[30] V. May and O. Kühn. *Charge and energy transfer dynamics in molecular systems.* John Wiley & Sons, Berlin, third edition, 2011.

[31] R. R. Valiev, V. N. Cherepanov, G. V. Baryshnikov, and D. Sundholm. First-principles method for calculating the rate constants of internal-conversion and intersystem-crossing transitions. *Phys. Chem. Chem. Phys.*, 20:6121–6133, 2018.

[32] M. Bixon and J. Jortner. Intramolecular radiationless transitions. *J. Chem. Phys.*, 48:715–726, 1968.

[33] V. G. Plotnikov. Regularities of the processes of radiationless conversion in polyatomic molecules. *Int. J. Quantum Chem.*, 16:527–541, 1979.

[34] A. I. Martynov, A. S. Belov, and V. K. Nevolin. A simplified bixon-jortner-plotnikov method for fast calculation of radiationless transfer rates in symmetric molecules. *Mol. Phys.*, 121:e2189981, 2022.

[35] M. Hayashi, A. M. Mebel, K. K. Liang, and S. H. Lin. Ab initio calculations of radiationless transitions between excited and ground singlet electronic states of ethylene. *J. Chem. Phys.*, 108:2044–2055, 1998.

[36] M. A. Krivoglaz and S. I. Pekar. The shape of the spectra of the impurity light absorption and luminescence in dielectrics. *Tr. Inst. Fiz. Akad. Nauk UKR SSR.*, 4:37–70, 1953.

[37] V. Vyas, P. Jain, and T. Nautiyal. Excess effective debye temperature of binary liquid mixtures from sound velocity measurements at 298 15k. *Indian J. Phys.*, 77:533–536, 2003.

[38] A. S. Vasudeva. *Textbook of Engineering Physics (Orissa).* S. Chand Publishing, 2008.

[39] T. J. Penfold and J. Eng. Mind the gap: quantifying the breakdown of the linear vibronic coupling hamiltonian. *Phys. Chem. Chem. Phys.*, 25:7195–7204, 2023.

[40] Code of the natrc programm. `https://github.com/Arthur140/NATRC`. Accessed: 2023-07-30.

[41] G. M. Barca, C. Bertoni, L. Carrington, D. Datta, N. De Silva, J. E. Deustua, D. G. Fedorov, J. R. Gour, A. O. Gunina, T. Guidez, E. Harville, S. Irle, J. Ivanic, K. Kowalski, S. S. Leang, H. Li, W. Li, J. J. Lutz, I. Magoulas, J. Mato, V. Mironov, H. Nakata, B. Q. Pham, P. Piecuch, D. Poole, S. Pruitt, A. P. Rendell, L. B. Roskop, K. Ruedenberg, T. Sattasathuchana, M. W. Schmidt, J. Shen, L. Slipchenko, M. Sosonkina, V. Sundriyal, A. Tiwari, J. L. G. Vallejo, B. Westheimer, M. Wloch, P. Xu, Zahariev F., and M. S. Gordon. Recent developments in the general atomic and molecular electronic structure system. *J. Chem. Phys.*, 152:154102, 2020.

[42] A. Dreuw and M. Head-Gordon. Single-reference ab initio methods for the calculation of excited states of large molecules. *Chem. Rev.*, 105:4009–4037, 2005.

[43] W. J. Stevens, M. Krauss, H. Basch, and P. G. Jasien. Relativistic compact effective potentials and efficient, shared-exponent basis sets for the third-, fourth-, and fifth-row atoms. *Can. J. Chem.*, 70:612–630, 1992.

[44] S. Hirata and M. Head-Gordon. Time-dependent density functional theory within the tamm–dancoff approximation. *Chem. Phys. Lett.*, 314:291–299, 1999.

[45] J. Tomasi, B. Mennucci, and R. Cammi. Quantum mechanical continuum solvation models. *Chem. Rev.*, 105:2999–3094, 2005.

[46] A. V. Marenich, C. J. Cramer, and D. G. Truhlar. Universal solvation model based on solute electron density and on a continuum model of the solvent defined by the bulk dielectric constant and atomic surface tensions. *J. Phys. Chem. B*, 113:6378–6396, 2009.

[47] Intel core i73770k processor 8m cache up to 3-90 ghz. `https://www.intel.com/content/www/us/en/products/sku/65523/intel-core-i73770k-processor-8m-cache-up-to-3-90-ghz/specifications.html`. Accessed: 2023-07-30.

[48] Intel core i7-3770k. `https://www.techpowerup.com/cpu-specs/core-i7-3770k.c1001`. Accessed: 2023-07-30.